RSC Advances

ROYAL SOCIETY OF CHEMISTRY

www.rsc.org/advances

RSC Advances

RSC Publishing

ARTICLE

Improved photo-luminescence behaviour of Eu^{3+} activated $CaMoO_4$ Nanoparticles via Zn^{2+} incorporation

B. P. Singh,[a*] Maheshwary,[b] P.V. Ramakrishna,[c] Saurabh Singh,[a] V. K. Sonu,[d] Santosh Singh,[e] P. Singh,[a] A. Bahadur,[f] R. A. Singh[b] and S. B. Rai[f]

tableCite this: DOI: 10.1039/x0xx00000x

Received 00th April 2015,
Accepted 00th April 2015

DOI: 10.1039/x0xx00000x

www.rsc.org/

Zn^{2+}(0, 2, 5, 7 and 10 at.%) co-doped $CaMoO_4$:$2Eu^{3+}$ nanophosphors have been synthesized via polyol method using ethylene glycol (EG) as both capping agent and reaction medium at 150 °C. From XRD analysis, all 900 °C annealed, Zn–co-doped $CaMoO_4$:Eu^{3+} have tetragonal scheelite phas Some extra phase evolution has been observed for ASP Zn doped samples. Intensity and crystallinity of XRD patterns increase as heat treatment increases to 900 °C. Valence state of the involved compositions (Zn co-doped $CaMoO_4$: Eu) was investigated by X-ray photoelectron spectroscopy (XPS) and found that Ca, Mo, Eu and Zn are in their +2, +6, +3 and +2 oxidation states, respectively. TG-DSC studies of the as-prepared samples corroborate their thermal stability. TEM study reveals that particles have spherical morphology. Photoluminescence studies have been studied under ~266, and 395 nm excitation wavelengths. Zn co-doping in $CaMoO_4$:Eu matrix, produces the high distortion and modify the crystal field around Eu^{3+} ion and improves the PL intensity. CIE co-ordinates of 900 °C annealed 10 at.% Zn co-doped $CaMoO_4$:Eu sample under 266 nm excitation is x = 0.64 and y = 0.35, which are closer to the standard of NTSC (x = 0.67 and y = 0.33). CCT values vary for ASP and annealed samples at different excitation wavelengths. These investigations reveal that Zn co-doped $CaMoO_4$:Eu^{3+} nanophosphors can be used as potential red emitting phosphor which is bottleneck in the advancement of LEDs at much lower cost.

1. Introduction

White light-emitting diodes (*w*-LEDs) are promising and suppose to be the next generation illumination affairs due to their high energy efficiencies, long lifetimes, good reliability and environmental friendliness compared to conventional incandescent lamps. It is well known that *w*-LEDs are produced by mixing red, green and blue (RGB) LEDs, combing a blue LED with a yellow phosphor of $(Y,Gd)_3(Al,Ga)_5O_{12}:Ce^{3+}$,or using near-ultraviolet (UV) LED-stimulated RGB phosphors. The major challenge in developing near-UVLEDs is to explore high efficient tri-color phosphors that possess an excitation wave-length matches well with the emission spectrum of the near-UVLED chips.[1-3] The current red phosphors based on Eu^{3+} activated oxides, sulphides and nitrides have disadvantages such as low reliability, high toxicity and luminous efficacy, compared with blue and green phosphors. Therefore, it is necessary and urgent to explore novel red-emitting phosphors that can be efficiently excited in the near UV range. The scheelite type structured molybdates have vast industrial applications such as scintillators, solid state lasers, fluorescent lamps and in photocatalysis. One of the most fascinating aspects is to generate white light from single phasic phosphor material.[4-6] Calcium molybdate, $CaMoO_4$ is a self activated blue-green host having phonon energy ~815 cm^{-1}.[7] Photoluminescence properties can be tuned by doping with different rare earth ions. In $CaMoO_4$ lattice, Ca atoms having 8 co-ordinations making [CaO_8] polyhedra while Mo atom having 4-co-ordiantion building [MoO_4] polyhedra.[7, 8] MoO_4^{2-} units in $CaMoO_4$ lattice have broad and intense absorption bands. This occurs due to charge transfer from oxygen to metal in the near UV region. A blue-green light emission is observed due to transition into MoO_4^{2-} units in lattice host. Eu^{3+}-doped $CaMoO_4$ phosphors can be efficiently excited in the near-UV region, spanning from 250 to 400 nm.[9] Yan et al. has been reported 3 times improvement in red emission intensity in $CaMoO_4$:Eu via Bismuth co-doping.[10] Recently it had been reported that enhancement in luminescent intensity in $CaMoO_4$:Eu and in Y_2WO_6:Ln (Ln=Sm, Eu and Dy) through Gd^{3+} co-doping.[11,12] A single-component white-light phosphor is normally produced by co-doping a sensitizer and an activator into the same host matrix. There were a few prominent investigations had been

performed to improve the luminescent properties of $CaMoO_4$ phosphor by co-doping of other metal ions. However, low efficacy of these nano-materials confined their generalised applications. Consequently, it will be of great interest to significantly enhance the emission intensity of phosphors in order to deploy their potential applications.

The energy transfer mechanism from a sensitizer to an activator such as Eu^{2+}/Mn^{2+}, Ce^{3+}/Mn^{2+}, and Ce^{3+}/Eu^{2+} couples has been investigated in many inorganic hosts, and an effective resonance-type multi polar interaction has been verified in $NaSr_4(BO_3)_3$: Ce^{3+}/, Mn^{2+}, $NaBa_4(BO_3)_3$: Ce^{3+}/Mn^{2+}, $Sr_3Sc(PO_4)_3$: Eu^{2+}/ Mn^{2+},$Sr_3B_2O_6$: Ce^{3+}, Eu^{2+},and so on. Moreover, some single-phase phosphors, such as $Ca_{10}K(PO_4)_7$:Eu^{2+}/ Mn^{2+}, $Ca_9Y(PO_4)_7$: Eu^{2+}/Mn^{2+}, $Ca_9Y(PO_4)_7$: Ce^{3+}/ Eu^{2+},and $Ca_9Y(PO_4)_7$: Ce^{3+}/Mn^{2+}, are used to improve the emission intensity for n-UV LED (light emitting diode) applications.[11, 13,14]Also an improvement in photo-luminescence intensity has been reported with co-doping of charge compensators such as Li^+, K^+, Na^+ and Bi^{3+} in phosphors or with SiO_2 coating over particle of phosphor. In this direction, non-radiative rates are reduced by either charge compensation, improve crystallinity or extent of decrease of surface dangling bonds/OH bonds by shell from inner core phosphor.[15]Su and their co-workers also reported the enhanced photoluminescence in $CaWO_4$ based red phosphor via Eu and Na co-doping.[16]

There are some reports on Zn doped nano-pohsophors for their improvement in photoluminescence intensity in literature[17-21] but no such study on Eu^{3+}–Zn^{2+} co-doped $CaMoO_4$ materials has been found to the best of our knowledge.

Many reports have been published on synthesis routes as well as luminescent properties of molybdates doped with different lanthanide ions. Synthesis routes such as solid state reaction, auto-combustion, sol-gel, and solvo-thermal for $CaMoO_4$ and/or Ln^{3+} doped $CaMoO_4$ in literature with the emphasis of controlling the crystal size, morphology, and the composition, which are crucial for a high quantum efficiency.[22] Among these polyol synthesis has been effectively been used to prepare the metal-nanoparticles. In this methodology, ethylene glycol (EG) is used as a capping agent at low synthesis temperature (~150 ºC). The use of poly alcohols, like ethylene glycol, as reducing agents for obtaining metallic nanoparticles has some advantages, as the by-products obtained during this process are ketones or carboxylic acids, which can be easily removed from the reaction mixture.[23]

Herein we have prepared a series of $CaMoO_4$ based red phosphor including $CaMoO_4$:Eu^{3+}(Eu^{3+}=2 at.%) and $Ca_{1-x-y}MoO_4$:xEu:yZn (x=2, y= 2, 5, 7 and 10 at.%). The detailed photoluminescence properties of Eu^{3+} doped $CaMoO_4$ with different concentration of Zn^{2+} ions that emit light in visible range were studied for ASP and 900 °C annealed samples. The detailed structural and downshifting phenomenon –and involved decay kinetics have been been studied as Zn co-doping in Eu^{3+} activated $CaMoO_4$ phosphor matrix.

2. Synthesis

Zn^{2+} (Zn^{2+} = 2, 5, 7 and 10 at.%) co-doped $CaMoO_4$:Eu (here concentration of Eu^{3+} is taken as 2 at.% optimal) prepared using ethylene glycol (EG) as capping agent and as well as reactio medium at 150 ºC. Zinc oxide (ZnO, AR grade), Calcium carbonate ($CaCO_3$, AR grade), Europium oxide (Eu_2O_3, 99.99%, Sigma Aldrich) and Ammonium Molybdate $(NH_4)_2Mo_7.4H_2O$, AR grade) were used as sources of Ca^{2+}, Eu^{3+} and MoO_4^{2-}. In a typical synthesis procedure of 1 g sample of 5 at.% Zn^{2+} co- doped $CaMoO_4$:Eu nanoparticles, 0.3312 g of $CaCO_3$ and 0.0189 g of Eu_2O_3 and 0.0146 g of ZnO were dissolved together in concentrated nitric acid (HNO_3). The mixture was heated at 80 ºC to remove the excess of acid and the process of removal of excess of acid was repeated five times after addition of de-ionized water (5 ml). To this solution 0.6351 g of $(NH_4)_2Mo_7.2H_2O$ was added followed by 50 ml of EG. The pH of the solution was adjusted to 8–9 using urea. The resulting solution was then stirred for 1 hour. This solution is then transferred to a two neck round bottom flask and was heated up to 150 ºC for 2 hours under refluxing condition in a condenser until precipitation was complete. The white precipitate so obtained was collected by centrifugation and washed 5 times in methanol to remove excess of EG and finally it was washed with acetone and dried at 90 ºC for 2 hours in ambient condition to yield the final white product. Finally, the as prepared samples were divided in 2 parts. One part of the sample was annealed at 900 ºC in an ambient atmosphere at a heating rate of 2 ºC min^{-1} for 4 hours in an alumina crucible and the other part was left untreated.

2.1 Characterization techniques

Phase confirmation of the synthesized samples was examined by Rigaku- Miniflex-II X-ray diffractometer. The chemical composition and valence state of the elements were analysed by X-ray photoelectron spectroscopy (XPS) using a monochromatic AlK_α (hυ =1486.6eV) X-ray source and a hemispherical analyzer (SPECS, HSA3500).The recorded spectra were charge-corrected to the C1s ~ 284.6 eV as the reference. The size and morphology of the samples were inspected using a Transmission Electron Microscope (TEM) JEOL JSM 100CX operating at an accelerating voltage of 200kV. The samples for TEM were prepared by depositing a drop of a colloidal ethanol solution of the powder sample onto a carbon-coated copper grid. Photoluminescence excitation (PLE), emission (PL) and lifetime measurements were performed using a Fluorolog-3 spectro-fluorometer (Model: FL3-11, Horiba Jobin Yvon). The 266 n excitation wavelength of a Nd:YAG laser and CCD (charged coupled device) detector (Ocean Optics, QE 65000) was also used for emission measurement.

3. Results and discussion

3.1 Structural studies

3.1.1 XRD study

XRD patterns of Zn^{2+} (0, 2, 5, 7 and 10 at.%) co-doped $CaMoO_4$:Eu ASP, and annealed at 900 °C samples has been shown in Fig.1(a) and (b). It is evident from the figure that even as-prepared (ASP) sample shows highly crystalline behaviour with tetragonal structure. However some extra peaks (marked as #) in ASP samples having smaller in intensity was observed for Zn co-doping at 2θ = 24.05, 26.26 and 28.57°. Peak intensity of these peaks increases with Zn doping. These peaks are not matching with JCPDS card no. 29-0351. These peaks evolution may be assigned to $MoO_n.mH_2O$ (m and n be the whole integers), other Eu-Mo-O related compounds present on the sample. Similar results have been reported for $CaMoO_4$ and $SrWO_4$ doped systems with Tb^{3+} and Eu^{3+}different activator ions. [22, 23]

All diffraction peaks for 900 °C annealed samples match well with JCPDS card no. 29:0351 (a = 5.226 Å, c = 11.43Å and V = 312.17Å^3). The lattice parameters of ASP 2 at.% Zn^{2+} -doped $CaMoO_4$ are a = 5.230 Å, c =11.462 Å, V = 313.56 Å^3 and 900 °C annealed samples are a = 5.231 Å, c =11.46 Å, V = 313.57 Å^3. Over all cell volume decreases on annealing the samples as compared to ASP samples with Zn^{2+} co-doping in $CaMoO_4$:Eu host matrix. The unit-cell constants and the calculated average crystallite sizes of the ASP and 900 °C annealed samples of $CaMoO_4$ with different concentrations of Zn^{2+} ions are summarized in Table S1 (ESI†).

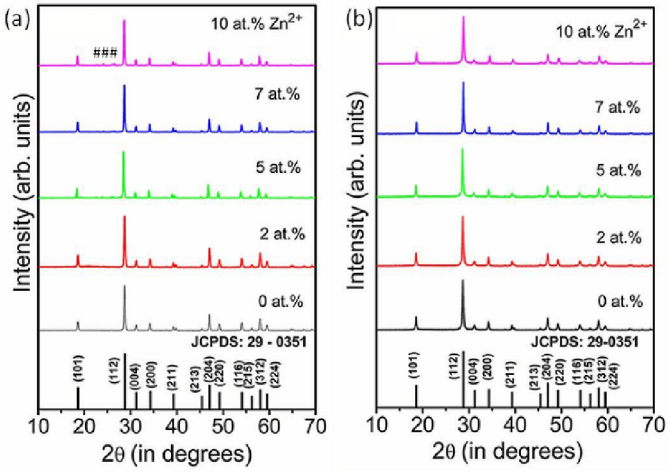

Fig.1 XRD patterns of Zn^{2+} (0, 2, 5, 7 and 10 at.%) doped $CaMoO_4$:Eu^{3+} nanoparticles for (a) ASP and (b) 900 °C annealed samples. Symbols marked as (#)shows the extra phase evolution.

The diffraction patterns intensity of 5, 7 and 10 at.% Zn^{2+} -doped $CaMoO_4$:Eu was found to be slightly less than 2 at.% doped samples which may be due to defects created at higher concentration in Zn^{2+}-doped $CaMoO_4$:Eu (Fig. 1(a)). Samples annealed at ~ 900 °C show slightly higher crystalline behaviour than the ASP samples, which is shown in Fig. 1(b).

The average crystallite sizes were estimated by the Scherrer formula,

$$D = \frac{k\lambda}{\beta\, Cos\theta} \qquad (1)$$

where, D is the average crystallite size, λ is the wavelength of the X-rays (1.5405 Å), and θ and β are the diffraction angle and full-width at half maximum (FWHM) of the peak in the XRD pattern, respectively. The strongest four peaks (1 0 1) at 2θ = 18.71, (1 1 2) at 2θ = 28.71, (2 0 0) at 2θ = 34.48 and (204) at 2θ = 47.10 were used to calculate the average crystallite size (D) of the powders. It can be seen that the lattice parameters and cell volume decrease as Zn^{2+} concentration increases from 2 to 10 at %. This is due to the substitution of Ca^{2+} (C.N=8, 1.12 Å) ions[7] by Zn^{2+} (C.N. =6, 0.74 Å) [24]and Eu^{3+} (1.06 Å) ions.[7]

The Rietveld analysis was performed for Zn (0, 2, 5, 7 and 10 at.%) co-doped $CaMoO_4$:Eu annealed at 900 °C using the *FullProf* software.[25] Typical rietveld fitting for undoped and 2 at.% Zn co-doped $CaMoO_4$:Eu has been shown in Fig. 2(a) and (b). The Wyckoff positions of atoms based on space group $I4_{1/a}$ (88) and Z = 4 (number of $CaMoO_4$ formula units per unit cell) in $CaMoO_4$ unit cell are: [7,8]

Ca: (4b: 0, 0.25, 0.0625),

Mo: (4a: 0, 0.025, 0.125)

and O: (16f: x, y, z) with angles (α=β=γ=90°).

Pseudo-Voigt function was used to model the peak profiles and six coefficient polynomial was used to describe the background.

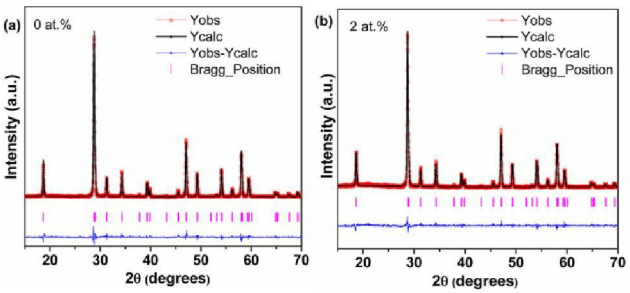

Fig. 2. Rietveld XRD patterns demonstrating observed, calculat difference and corresponding Braggs positions of (a) un-doped and (b) 2 at.% Zn co-doped $CaMoO_4$:Eu.

3.1.2 TEM Study

Fig. 2 illustrates the TEM micrograph of 10 at.% Zn doped $CaMoO_4$:Eu nano-particles annealed at 900 °C. Most of the

nano-particles have irregular shapes and a few have the spherical shape. It is well known that the uniformity of the size and shape is controlled by nucleation.[23] In polyol synthesis, reaction was started after adding ethylene glycol.

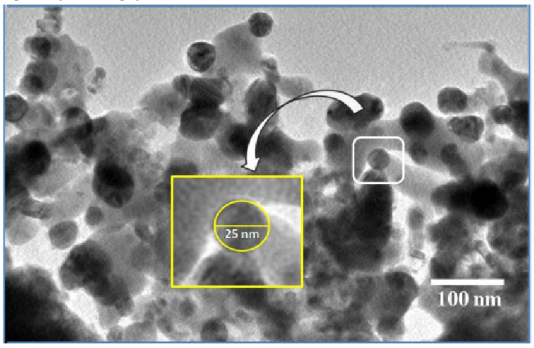

Fig.3. TEM micrograph of 10 at.% Zn co-doped $CaMoO_4$:Eu annealed at 900 °C sample.

ASP samples show high agglomeration (shown in Fig S1 (ESI†) and Zn inclusion improves the grain growth of the particles shape evolution. During the heating process, nucleation and crystal growth processed. This results irregular shapes and agglomerated particles.[26] The particle sizes estimated from TEM is ~25-52 nm, which is in agreement with the calculated sizes from XRD studies. Typical particle size estimated (shown in Fig. 3 itself) has been estimated to be ~25 nm.

3.1.3 DSC/TGA Study

Fig.4 shows the simultaneous DSC/TGA curves along with DTG curves of ASP 2 at.% Zn^{2+} co-doped $CaMoO_4$:Eu^{3+} sample. The sample was measured in the temperature range of 35 to 800 °C with a heating rate of 10 °C/min under nitrogen atmosphere. In the TG curve, a weight loss of ~11% between 80 to 250 °C, 1.35% in the range 250-600 °C and no appreciable loss was observed beyond 600 °C. There is having marginal weight loss observed in vicinity of around 650 (TG/DTG curve) which may be due to artefact. Also similar observations have been reported in literature.[27, 28] The mass loss till 300 °C is attributed to complete dehydration of the powders while the mass loss till 600 °C is due to the evaporation of organic constituents like EG and methanol.

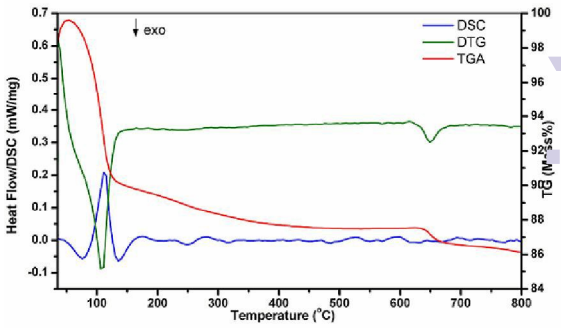

Fig.4 Simultaneous DTG/TGA and DSC isotherms of 2 at.% ASP Zn^{2+} co-doped $CaMoO_4$:Eu^{3+}.

To study the heat flow as a function of temperature in the inert gas (N_2) atmosphere associated with transitions in 2 at.% Zn^{2+} co-dop $CaMoO_4$:Eu^{3+}ASP sample DSC was recorded (Fig.4). The cur show only endothermic peaks. The peak around 110 °C represents the mass loss due to evaporation of water and methanol. These results show that the prepared nano-phosphors are thermally stable and can be used in lightning and display devices.

3.1.4 Raman Study

Fig.5 show the Raman spectra for Zn^{2+} (0 and 10 at.%) co-doped $CaMoO_4$:Eu^{3+} sample annealed at 900ºC. The Scheelite structure shows 26 modes of vibrations (3Ag, 5Au, 5Bg, 3Bu, 5Eg, 5Eu) in which 13 modes are Raman active (3Ag, 5Bg, 5Eg) and (4Au, 4Eu) are IR active. The three B_u vibrations are silent modes whereas one A_u and one E_u modes are acoust vibrations.[7, 29] Eight Raman-active modes were observed in the Raman spectrum and the other ($3B_g$ and $2E_g$) vibration modes were not detectable, this may be due to their low intensities. However, due to strong interaction between the O-Ca-O and O-Mo-O bonds in the clusters, the Raman spectra exhibited intense and sharp bands.[30, 31] Strong intense bands at 875, 843, and 791 cm^{-1} are attributed to the A_g, B_g and E_g modes, respectively. Bands at 202 and 389 cm^{-1} can be attributed to the B_g and A_g modes. The band at 320 cm^{-1} is the superposition of A_g (ν_2) and E_g (ν_2) modes of vibrations. The three E_g internal modes are observed at 791, 139 and 107 cm^{-1}. The four Raman bands below 267 cm^{-1} are due to external modes (lattice modes) whereas the five bands below 920 cm^{-1} correspond to internal/optical modes (within MoO_4^{2-}).[32]

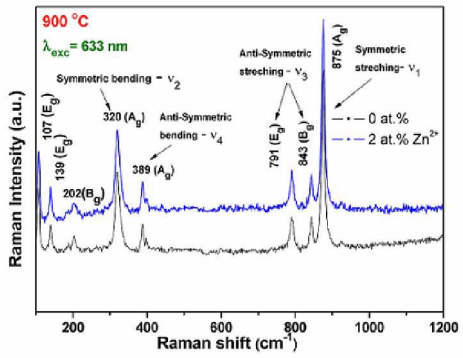

Fig. 5. Room temperature Raman spectra of Zn free and 10 at.% Zn co-doped $CaMoO_4$:Eu samples annealed at 900 °C.

All Raman –active modes of $CaMoO_4$ crystals reported in this work are in good agreement with those reported in literature.[33,34] In fact, the shifts observed on these bands can be attributed to the degree of interaction between the O-Mo-O bonds and distortions on the [MoO_4] clusters induced by the structural order disorder in the lattice.

3.1.5 XPS study

The compositional and chemical state of the Zn (0, 2, 5, 7 and 10 at.%) co-doped $CaMoO_4$:Eu samples, has been examined by X-ray photoelectron spectroscopy (XPS). XPS spectra of Ca, Mo, O and Zn for Zn (0, 2, 5, 7 and 10 at.%) co-doped $CaMoO_4$:Eu is shown in Fig. 6. XPS survey spectrum for 5 at.% Zn doped $CaMoO_4$:Eu sample at 900 °C comprising core BE levels of Ca, Mo, O, Eu/Zn is shown in Fig. S2(ESI†) obtained in the range of 0-1100 eV. Fig. 6(a) shows the XPS spectrum of Ca (2*p*) for 0, 2, 5, 7 and 10 at.% Zn^{2+} co-doped $CaMoO_4$:Eu ASP samples. For Zn^{2+} free $CaMoO_4$:Eu sample, the peaks are corresponding to Ca (2*p*) having core BE ~346.64 ($2p_{3/2}$) and 350.19 eV ($2p_{1/2}$) and corresponding full width at half maximum (FWHM) ~1.7 and 2.0 eV. Peaks were convoluted using Gaussian function. Typical fitting of Ca2p spectra has been shown in Fig.S3(ESI†). On increasing Zn^{2+} (0, 2, 5, 7 and 10 at.%) co-doping concentration, there is slight changes in BE values to higher eV. Moreover, integrated intensity ratio of ($2p_{3/2}$) to ($2p_{1/2}$) (I_{Ca}) is found to be 1.71, 1.79, 169, 1.51 and 1.41 for 0, 2, 5 7 and 10 at.% Zn^{2+} co-doping, respectively. These results confirm +2 oxidation state of Ca. Fig. 6(b) shows the peaks at ~232.39 and 235.53 eV, which correspond to the core BE of Mo($3d_{5/2}$) and Mo($3d_{3/2}$), respectively for 900 °C Zn^{2+} free $CaMoO_4$:Eu sample. Integrated intensity ratio of ($3d_{5/2}$) to ($3d_{3/2}$) (I_{Mo}) are found to be 1.31, 1.37, 1.41, 1.49 and 1.39 for 0, 2, 5, 7 and 10 at.% Zn^{2+} co-doping samples, respectively (Fig. 6(b)). There is no significant change in BE on Zn^{2+} co-doping. Also, (I_{Mo}) found to be 1.39, 1.32, 1.38, 1.43 and 1.39 for 0, 2, 5, 7 and 10 at.% Zn^{2+} co-doping samples, respectively. The lack of any significant change in the $3d_{3/2}$-$3d_{5/2}$ BE in the Mo spectral region suggests that Mo ions remain in its Mo^{6+} state.[7] Similar behaviour was supported in literatures for Ca Bi-Mo oxide and for the molybdenum phosphate glass.[35] Typical fitting of Mo3d spectrum has been shown in Fig. S4 (ESI†).

Peak at ~141.1 eV, which corresponds to Eu^{3+}($4d_{3/2}$) and there having no peak at ~127.1 eV corresponding to Eu^{2+}($4d_{5/2}$) is observed. This confirmed the high probability of Eu^{3+} in the sample (Shown in Fig.S5(ESI†). It is also confirmed from photoluminescence study (discussed later). Typical XPS spectrum of Eu^{3+} showing core binding energy and intensity with Zn (0, 2 and 10 at.%) co-doped $CaMoO_4$:Eu at 900 °C samples is shown in Fig. S5(ESI†). Intensity of these peaks is very small for 900 °C annealed samples and improves with increase of Zn^{2+} concentration.

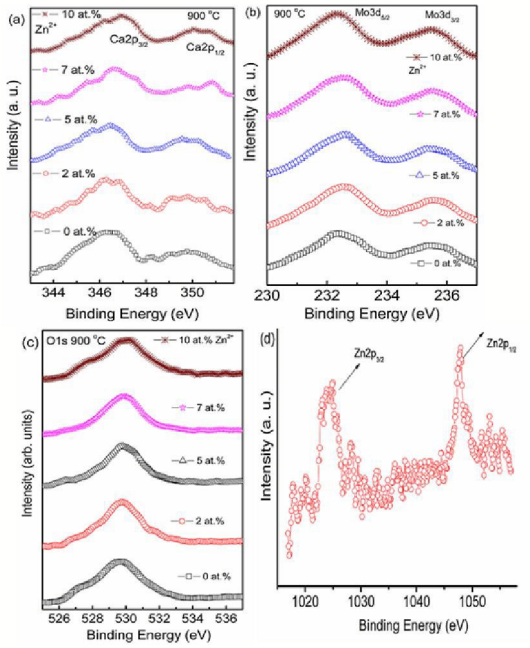

Fig.6. XPS spectra of (a) Ca (2p) (b) Mo (3d) (c) O (1s) and (d) Zn (2p).

In addition, O(1s) spectral regions have been used to obtain the information regarding the presence of oxygen vacancies present in the sample (Fig. 6(c)). Peaks were de-convoluted using Gaussian function. Two peaks are well fitted at BE ~ 529.7 (P_1) and 531.43 eV (P_2) having FWHM ~1.7 and 1.79 eV, respectively. Typical peak fitting of O1s spectra for 10 at.% Zn doped at 900 °C annealed sample has been shown in Fig.S6(ESI†). On increasing Zn^{2+} co-doping peak position slightly changes by ± 0.1-0.2 eV (Fig. 6(c)). Overall peaks show asymmetric nature in higher BE side. This is may be due to the defects and of oxygen vacancies creation on behalf of Zn^{2+} doping. There are few reports which indicate that high

energy side of O(1s) peak arises due to hydroxyl groups –OH or other radicals on the sample surface as CO or CO_2.[36]However, the asymmetric behaviour at high energy peak (~530.5 eV) in an O1s spectrum is signature of the presence of oxygen ion vacancy in the lattice.[37]Vacancies decreases on annealing from the sample surface.[7] It was observed the Core BE peaks of 10 at.% Zn doped $CaMoO_4$:Eu at ~1024.56 and ~1048.4 eV corresponds to $Zn2p_{3/2}$ and $Zn2p_{1/2}$ (Fig.6(d)).[38]

4. Optical Studies

4.1 Excitation Study

Excitation spectra of ASP Zn co-doped (0, 2, 5, 7, and 10 at.%) $CaMoO_4$:Eu nano-phosphors at 615 nm emission wavelength has been shown in Fig.7. A broad band from 230 to 320 nm is observed which arise due to the combination of the ligand to metal charge transfer $O^{2-}\rightarrow Mo^{6+}$ and charge transfer band (CTB) from the completely filled 2p orbitals of O^{2-} to the partially filled f-f orbitals of the Eu^{3+} ions ($O^{2-}\rightarrow Eu^{3+}$) .[9, 22, 32] and the intra f-f transitions of Eu^{3+} around 360 ($^7F_0 \rightarrow {}^5D_4$), 376 nm ($^7F_0 \rightarrow {}^5G_3$), (382 ($^7F_0 \rightarrow {}^5G_4$), 395 ($^7F_0 \rightarrow {}^5L_6$), 415 ($^7F_0 \rightarrow {}^5D_3$), 464 ($^7F_0 \rightarrow {}^5D_2$) and 532 nm ($^7F_0 \rightarrow {}^5D_1$) are observed. The wavelength corresponding to the peak of Eu/Mo -O CT band around 230-320 nm decreases from 280 to 266 nm and the corresponding FWHM decreases from 51 to 37 nm with the increase in Zn^{2+} ion concentration upto 2 at.%. This blue shift in the Mo/Eu-O CT band with Zn^{2+} ion concentration can be related to some Mo/Eu based compound formation which may results in phase segregation.(also observed from ASP XRD data of Zn doped samples). The excitation spectra of 900 °C annealed Zn co-doped (0, 2, and 10 at.%) $CaMoO_4$:Eu^{3+} nano-phosphors at 615 nm emission wavelength has been given in Fig.S7 (ESI†).

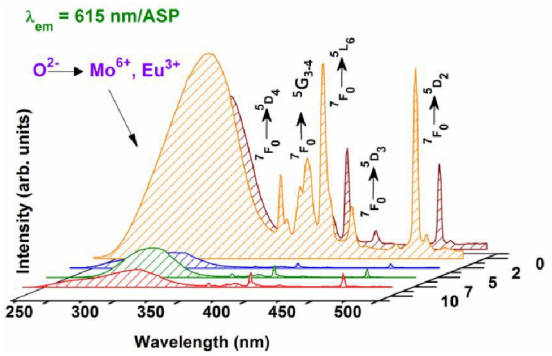

Fig.7. Excitation spectra of ASP, Zn (0, 2, 5, 7 and 10 at.%) co-doped $CaMoO_4$:Eu samples monitoring emission at 615 nm wavelength.

The intensity of bands increases upto 10 at.% Zn^{2+} co-doping and position of Eu/Mo-O charge-transfer band (CTB) is shifted to higher wavelength by ~ 2-5 nm due to annealing of the samples at 900 °C than in ASP samples; similar observations have been reported in Mo–O CTB in $CaMoO_4$ and W-O CTB in CaWO4 host.[29, 32]

When an electron is transferred from oxygen to Mo, an electronic transition takes place which gives rise to the Mo–O charge transfer band (CTB). In ASP samples, there are a relatively large number of dangling bonds over the particle surface and the lattice is less ordered as compared to that of annealed samples. There is also a higher degree of ionic character between Mo and O for the as-prepared samples as compared to that for 900 °C annealed samples, and this result in lower energy absorption for annealed samples. On annealing the degree of co-valent character increases Consequently, the position of the Mo–O charge-transfer band is shifted to higher wavelength by ~2-5 nm upon annealing the samples as compared to the as-prepared samples.[28]

4.2 Emission Study

Eu^{3+} ion has generally been selected as the activator ion to investigate the luminescence properties of rare earth tungstate/molybdate materials as it shows emission in the visible region. Since ground electronic state configuration of Eu^{3+} ion has $^7F_0$ non degenerate and having non-overlapping $^{2S+1}L_J$ multi-plets. Therefore Eu^{3+} ion can be used as a structural probe for investigating the local environment in a host matrix.[39] It is well documented that the symmetry of the crystal sites of doped Eu^{3+} ions will determine the relative intensity of the $^5D_0\rightarrow{}^7F_1$ and $^5D_0\rightarrow{}^7F_2$ transitions. If the $^5D_0\rightarrow{}^7F_1$ magnetic dipole transition is dominant in the spectrum, this indicates that europium is located in a site with inversion symmetry. If the $^5D_0 \rightarrow{}^7F_2$ electric dipole transition is dominant this means that $Eu^{3+}$is located in a site without inversion symmetry.[40]

Fig.8 (a) shows the PL emission spectra of ASP Zn (0, 2, 5, 7 and 10 at.%) co-doped $CaMoO_4$:Eu^{3+} under 266 nm excitation. All the samples show strong $^5D_0 \rightarrow{}^7F_2$ (615 nm), $^5D_0 \rightarrow{}^7F_1$ (590 nm), $^5D_0\rightarrow{}^7F_3$ (654nm) and $^5D_0\rightarrow{}^7F_4$ (705 nm) emission lines upon 266 nm excitation. It is observed that electric dipole transition at 615 nm is dominant over magnetic dipole transition at 590 nm. It is well documented that electric dipole transition is hypersensitive to its environment and parity allowed transition originating from $^5D_0\rightarrow{}^7F_1$ is insensitive to the crystal field environment. It is suggested that most of the Eu^{3+} enters into the lattice sites having centre without inversion symmetry.[11, 23, 40] Emission intensity increases upto 2 at.% Zn^{2+} doped $CaMoO_4$:Eu may be due to substitutinal and crystal field effect. After 2 at.% Zn doping, intensity decreases. Zn^{2+} co-doping may create the vacancies that act as the sensitizer, mixing the charge-transfer states. Zn^{2+}addition increased the PL intensity by increasing the radiative transition probability. However, an increase in the Zn^{2+} Concentration over a certain limit generates a significant amount of oxygen ion vacancies in the lattice. Consequently, the crystal lattice collapses, and the luminescence intensity decreases.[42]

Similar behaviour has been reported for Li^+ doped system.[43] PL bands positions but having different luminescence intensity has been observed for 900 °C annealed samples as compared to ASP Zn doped samples (shown in Fig.8(b)). Addition of 10 at.% Zn^{2+} in $CaMoO_4$:Eu annealed at 900 °C sample, photoluminescence intensity increases ~3 times as compared to without Zn^{2+} doping $CaMoO_4$:Eu at 900 °C. Emission intensity increases upto 10 at.% Zn^{2+} doping. On annealing the samples crystallinity increases, decreases non-radiative decay and the vacancies and the asymmetric ratio is improved. It means that co-doping of Zn^{2+} improves luminescence. Improvement of luminescence is due to the substitution of Ca^{2+} sites by Zn^{2+} ions. Zn^{2+} doping may change the crystal field and asymmetricity around

Eu^{3+} ion which leads electric dipole transitions. Also the energy absorbed by the Zn^{2+} fully or partly transferred into Eu^{3+}, raising the activation energy of Eu^{3+} and increasing the transition processes, leading to the improvement of the emitting intensity and red color purity. It is likely that the dipole moment of the transitions increases upon co-doping of Zn^{2+} ions. In addition, improved crystallinity as well as removal of organic moiety (such as PEG) gives rise to enhance luminescence after heat treatment at 900 °C. Also PL study of Zn doped $CaMoO_4$:Eu for ASP and annealed at 900 °C samples under 395 nm excitation has been measured and it showed similar pattern intensity as under 266 nm excitation. [Shown in Fig.S8 and Fig.S9 (ESI†)]

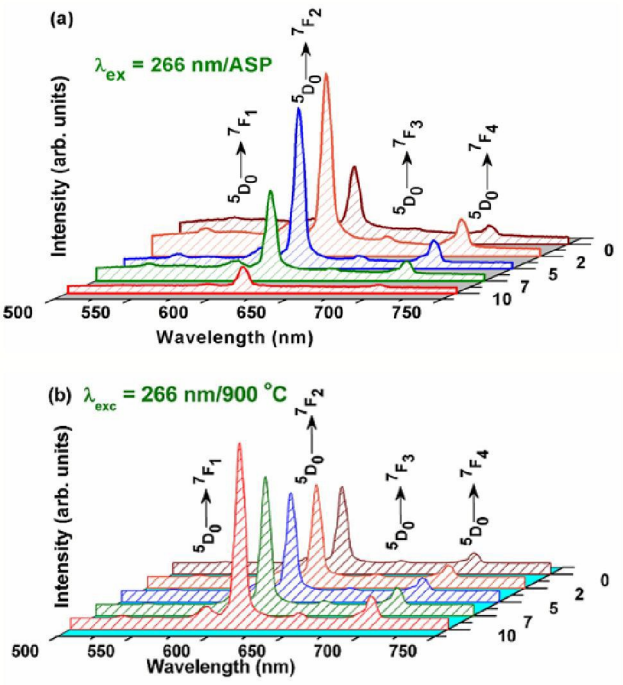

Fig.8. Emission spectra of Zn^{2+} (0, 2, 5, 7 and 10 at.%) co-doped $CaMoO_4$:Eu for (a) ASP and (b) 900 °C annealed samples at 266 nm excitation wavelength.

The ratio of integrated area of electric dipole transition ($^5D_0 \rightarrow {}^7F_2$) to magnetic dipole transition ($^5D_0 \rightarrow {}^7F_1$) has been probed to study the structural distortion around the Eu^{3+} ion, is known as asymmetric ratio (A_{21}).[11, 23] In our case the asymmetric ratio is represented as,

$$A_{21} = \frac{\int_{600}^{630} I_2 d\lambda}{\int_{580}^{600} I_1 d\lambda} \qquad (2)$$

where subscript '2' and '1' refer to transitions of $^5D_0 \rightarrow {}^7F_J$, j=2 and 1, respectively. Value of A_{21} for ASP Zn (0, 2, 5, 7 and 10 at.%), co-doped samples is ~7.4, 9.8, 8.5, 8.1 and 7.4. The value of A_{21} for Zn (0, 2, 5, 7 and 10 at.%) co-doped samples annealed at 900 °C is 7.8, 8.7, 9.2 and 10.6. Higher values of A_{21} clearly demonstrates that Eu^{3+} occupy site without inversion symmetry. Overall, the A_{21} values increase on annealing because of decrease of non-radiative rates. The increase in A_{21} values demonstrates high distortion present in the host lattice which shows high red emitter.[11, 23, 40, 41]

4.3 Decay Analysis

The decay curves of the level $^5D_0$ (615 nm) of Eu^{3+} has been measured and shown in Fig.9. The excitation wavelength is fixed at 395 nm. The decay curves for Eu^{3+} emission can be well fitted by using bi-exponential curve fitting which is expressed as:

$$I = I_1 e\left(\frac{-t}{\tau_1}\right) + I_2 e\left(\frac{-t}{\tau_2}\right) \qquad (3)$$

Where I_1 and I_2 are the intensities at different time intervals τ_1 and and τ_2 are their corresponding lifetimes. The bi-exponential fitting of 10 at % Zn^{2+} doped as-prepared and 900 °C $CaMoO_4$:Eu phosphor under 395 nm excitation are shown in Fig. 9 (a) and (b). Decay profile has been recorded monitoring the emission at 615 nm at 395 nm excitation (direct excitation of Eu^{3+}). Decay profile shows its bi-exponential behaviour. It corroborates that availability of Eu^{3+} ion on the surface (τ_1) and core (τ_2) of the particles. Further, the average decay life times can be calculated as:

$$\tau_{av} = \frac{I_1\tau_1 + I_2\tau_2}{I_1 + I_2} \qquad (4)$$

The life time values obtained using bi-exponential decay equation for ASP and 900 °C annealed 10 at.% Zn^{2+} co-doped $CaMoO_4$:Eu are ~0.58 and 0.76 ms, respectively under 395 nm excitation.

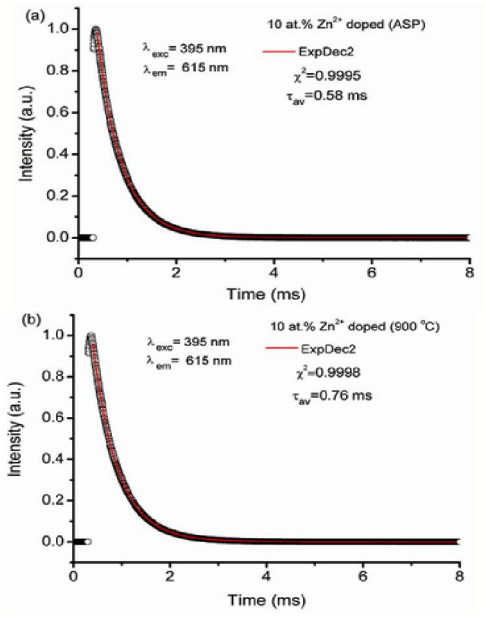

Fig. 9. Decay curve of 10 at.% Zn co-doped $CaMoO_4$:Eu (a) ASP and (b) 900 °C annealed sample under 395 nm excitation.

These values are in good agreement with the reported values for other Eu^{3+} doped compounds.[9, 11] As for Mo-O CTB (~266 nm) excitation, luminescence decay follows non-exponential equation because at initial stage energy transfer from Mo-O or Zn^{2+} to the excited states of Eu^{3+} occurs and then the decays form $^5D_0$ level. The details of energy transfer rate and mechanism were reported in literature.[11, 22]. In case of annealed samples at 900 °C, the lifetime values are higher than that of as-prepared samples. This may be due to reduction in non-radiative rates R_0 as compared to radiative rate. Non radiative rate R_0 is expressed as :

$$R_0 = \alpha e^{-(\Delta E - 2h\nu_{max})\beta} \quad (5)$$

Where α and β are constants. ΔE is the difference in energy between excited and ground states of the activator (Eu^{3+}) ions, ν_{max} are the highest available vibrational modes of the surroundings of the rare earth ion. In case of Eu^{3+} ion, ΔE is ~10000-15000 cm^{-1} and the value is comparable with the third overtone stretching vibrations of –OH functional group (~3500 cm^{-1}). This functional group arises from the water molecules absorbed or associated during the synthesis of nanomaterials. EG and aqueous medium are used and are source of water. The R_0 value becomes large when $\Delta E \sim 2h\nu_{max}$. In case of ASP samples, significant extent of nonradiative transfer of energy from excited states of Eu^{3+} ions to the different vibrational modes of –OH species occurs which leads to reduction in Eu^{3+}emission. Similar report has been documented for Eu^{3+}/Mn^{2+} doped CaF_2 and Fe_3O_4 hybrid structure.[44] Recently the radiative and nonradiative decay rates of CdSe nanorods are found to be modified in Au/CdSe tetrapod structures and the nonradiative rate changes from $1.91 \times 10^7\ s^{-1}$ to $9.33 \times 10^9\ s^{-1}$ for CdSe nanorod to Au/CdSe tetrapod structure.[45]

The radiative decay rate constants are defined as:[11]

$$(k_r) = 1/\tau_{av} \quad (6)$$

Calculated values of radiative rate constants for 10 at% Zn^{2+} co-doped $CaMoO_4:Eu^{3+}$ for ASP and 900 °C are 1.724 $X10^3$ and 1.315 $X10^3\ s^{-1}$, respectively.

4.4 CIE study

Fig.10 shows the Commission Internationale de l'Eclairage (CIE) chromaticity diagram for Zn^{2+} (0 and 10 at.%) co-doped $CaMoO_4:Eu^{3+}$annealed at 900 °C phosphors excited at 266nm. CIE coordinates varies for ASP and 900 °C annealed samples. Typical CIE coordinates for 10 at.% ASP Zn^{2+} co-doped sample is (0.47, 0.40). CIE color coordinates for Zn free and 10 at.% Zn^{2+} co-doped $CaMoO_4$:Eu annealed samples at 266 nm excitation is (0.58, 0.36) and (0.64, 0.35), which lie well in the red region. It is worthwhile to observe that under 266 nm excitation, the color coordinates are located in the blue region for ASP samples and lie in red-light region, for 900 °C annealed samples. Blue emission color contribution may be due to host emission while red emission is the characteristic region for emissions from Eu^{3+}. Detailed CIE coordinates have been calculated for Zn co-doped samples for ASP and annealed at 900 °C under 266 nm excitation, given in Table S2 (See ESI†).

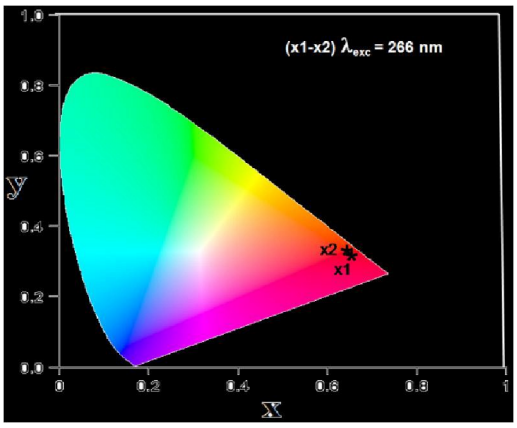

Fig.10 CIE diagram of Zn^{2+} free and 10 at.% Zn^{2+} co-doped $CaMoO_4$:Eu annealed at 900 °C.

4.5 CCT Study

The quality of white light has been estimated using McCamy empirical relation in terms of Color Correlated Temperature (CCT) values, which is expressed as:[23]

$$CCT = -449n^3 + 3525n^2 - 6823n + 5520.33 \quad (7)$$

where, $n = (x - x_e)/(y - y_e)$ is the inverse slope line, $x_e = 0.332$ and $y_e = 0.186$.

The CCT values for as-prepared and 900 °C annealed samples are found to be in the range of ~1703-3824 K for different Zn^{2+} ion concentrations under266 nm excitation. The typical CCT value for 900 °C annealed 5 at.% Zn^{2+} co-doped sample under 266 nm excitation is found to be 2508 K (warm white light). It suggests that color temperature of Zn^{2+} co-doped $CaMoO_4:Eu^{3+}$ nanophosphors can be manipulated by changing the Zn^{2+} concentration and by annealing the samples. The detailed CCT values for ASP and annealed samples at 900 °C for different Zn concentrations under 266 and 395 nm excitation wavelengths are given in Table S3 (See ESI†).

5. Conclusions

Highly nano-crystalline nanoparticles of Zn co-doped $CaMoO_4$:Eu has been prepared using polyol synthesis. Tetragonal scheelite single phase has been confirmed through XRD study. Characteristics valence states for Ca, Mo, Zn and Eu have been probed through XPS study and these were in its formal +2, +6, +2 and +3 oxidation states. TEM study confirms the spherical morphology of the Zn doped samples. Characteristic Raman modes of vibrations have been observed for $CaMoO_4$ host. Enhanced photoluminescence for 900 °C annealed samples has been

observed as compared to ASP via Zn-doping, it may be due to the reduction of –OH ions and organic moieties at higher temperature. Also Zn^{2+} co-doping in $CaMoO_4$:Eu matrix produces high assymetricity. Asymmetric ratio is ~7.4 to 10.6 which reflects it as a high red emitter. Zn^{2+} co-doping favours the crystallinity and changes the crystal field around Eu^{3+} ion, results a significant enhancement in PL intensity. CIE coordinates for ASP lie in blue region while for annealed samples, it lie in red region. Quality of white light can be manipulated by Zn co-doping and annealing of the samples. Its CCT values varies for ASP and 900 °C Zn^{2+} co-doped $CaMoO_4$:Eu samples. The typical CCT value for 900 °C annealed 5 at.% Zn^{2+} doped sample under 266 nm excitation is found to be 2508 K (warm white light). Studies corroborate the potentiality of these samples as a promising red phosphor for w-LEDs applications.

Acknowledgements

One of the authors BPS is thankful for financial assistantship to Council of Scientific and Industrial research (CSIR), New Delhi, India for providing the Senior Research Fellowship. Also author Maheshwary acknowledges the Central Research Fellowship provided by University Grants Commission (UGC), India. BPS gratefully acknowledges Dr. R. S. Ningthoujam, Chemistry Division, BARC, India for his support and encouragements.

Notes and references

*Corresponding Author: bheeshmapratap@gmail.com, bpsingh.rs.app@iitbhu.ac.in

[a]Department of Physics, IIT (BHU), Varanasi-221005, India.
[b]Department of Physics, Dr. H. S. Gour Central University, Sagar-M. P.-470003, India.
[c]Department of Physics, Andhra University,Visakhapatanam-530003,.India.
[d]Centre for Advanced Studies in Chemistry, North Eastern Hill University, Shillong-793022, India
[e]Department of Pure and Applied Physics, Guru Ghasidas University, Bilaspur, India-495009.
[f]Department of Physics, Banaras Hindu University, Varanasi-221005, India.

Electronic Supplementary Information (ESI) available:. See DOI: 10.1039/b000000x/

References:

[1]S. Neeraj, N. Kijima and A.K. Cheetham, Chem. Phys. Lett., 2004, 387, 2–6.
[2]G. S. R. Raju, H. C. Jung, J. Y. Park, B. K. Moon, R. Balakrishnaiah, Jeong J. H., Kim J. J. H., Sens. Actuators B, 2010, **146**, 395-402.
[3]M.Yamada, T. Naitou, K. Izuno, H. Tamaki, Y. Murazaki, M. Kameshima and T. Mukai, Jpn.J.Appl.Phys.,2003, **42**, 20–23.
[4]L. S. Cavalcante, V. M. Longo, J .C. Sczancoski, M. A. P. Almeida, A. A. Batista, J. A. Varela, Mo. O. Orlandi, E. Longo and M. S. Liu, Cryst. Eng. Comm., 2012, **14**,853–868.
[5]V. M. Longo, L. S. Cavalcante, E. C. Paris, J. C. Sczancoski, P. S. Pizani, M. S. Li, J. Andres, E. Longo and J. A. Varela, J. Phys. Chem. C, 2011, **115**, 5207-5219.
[6]J. Guo, D. Zhou, Y. Li, T. Shao, Z.-M. Qi, B. -B. Jinc and H. Wang, Dalton Trans., 2014, **43**, 11888-11896.
[7]B. P. Singh, A. K. Parchur, R. S. Ningthoujam, A. A. Ansari, P. Singh and S. B. Rai, Dalton Trans., 2014, **43**,4770-4778.
[8]A. K. Parchur and R. S. Ningthoujam, Dalton Trans., 2011, **40**, 7590-7594.
[9]A. K. Parchur, R. S. Ningthoujam, S. B. Rai, G. S. Okram, R.A. Singh, M. Tyagi, S. C. Gadkari, R. Tewari and R. K. Vatsa, Dalton Trans., 2011, 40, 7595-7601.
[10]S. Yan, J. Zhang, X. Zhang, S. Lu, X. Ren, Z. Nie and X. Wang, **J.** Phys. Chem. C, 2007, **111**, 13256-13260.
[11]B. P. Singh, A. K. Parchur, R. S. Ningthoujam, A. A. Ansari, P. Singh and S. B. Rai, Dalton Trans., 2014, **43**,4779-4789.
[12]A. M. Kaczmarek, K. V. Hecke and R. V. Deun, Inorg. Chem., 2014, **53**, 9498-9508.
[13] N. Guo, Y. Jia, W. Lü, W. Lv, Q. Zhao, M. Jiao, B. Shao and H. You, Dalton Trans., 2013, 42, 5649-5654.
[14] C. K. Chang and T. M. Chen, Appl. Phys. Lett., 2007, 91, 081902-1-3.
[15]A. Xie, X. Yuan, S. Hai, J. Wang, F. Wang and L. Li, J. Phys. D: Appl. Phys., 2009, 42, 105107-1-7.
[16]Y. G. Su, L. P. Li and G. S. Li, Chem. Mater.,2008, **20**, 6060–6067.
[17] R. Dey, V. K. Rai and A. Pandey, Spectrochim.Acta,PartA, 2012, **99**, 288-291
[18]V.Singh,V. K. Rai, I. Ledoux-Rak, L. Badie and H.Y. Kwak, Appl. Phys. B, 2009, **97**, 805-809
[19] A. Pandey and V. K. Rai, Dalton. Trans., 2013, 42, 11005-11011.
[20] S. M. Chung, S. Y. Kang, J. H. Shin ,W. S. Cheong, C. S. Hwang, K. I. Cho, S. J. Lee and Y. J. Kim, J. Cryst. Growth., 2011, **326**, 94-97
[21] D. Hartnath, A. F. Khan and H. Chander, J. Phys. D., Appl. Phys., 2006, **39**, 4956-4960.
[22]A. K. Parchur, A. I. Prasad, S. B. Rai, A. A. Ansari and R. S. Ningthoujam, Dalton Trans., 2012, **41,** 11032-11045.
[23]Maheshwary, B. P. Singh, J. Singh and R. A. Singh, RSC Adv. 2014, **4**, 32605-32621.
[24]R. D. Shanon, ActaCrystallogr., Sect. A: Cryst. Phys., Difr., Theor. Gen.Crystallogr.,1976, **32**,751.
[25]J. R. Carvajal, Introduction to the program FullProf, Laboratoire Leon Brillouin (CEA-CRNS), France.
[26]N. S. Gajbhiye and R. S. Ningthoujam, Mater. Res. Bull., 2006, 41, 1612-1621.
[27]N. V. Jadhav, A. I. Prasad, A. Kumar, R. Mishra, S. Dhara, K. R. Babu, C. L. Prajapat, N. L. Misra, R. S. Ningthoujam, B. N. Pandey and R. K. Vatsa, J. Colloids and Surface B:Biointerfaces, 2013, **108**, 158-168.
[28]M. N. Luwang, R. S. Ningthoujam, S. K. Srivastava and R. K. Vatsa, J. Am. Chem. Soc., 2011, **133**, 2998-3004.
[29]Maheshwary, B. P. Singh and R. A. Singh, New. J. Chem, 2015, **DOI:** 10.1039/C4NJ01911C.
[30]A. Golubovic, R. Gajic, Z. D.-Mitrovic, S. Nikolic, J. Alloy. Compd. 2006, **415**, 16-22.
[31]Z. C. Ling, H. R. Xia, D.G. Ran, F. Q. Liu, S. Q. Sun, J.D. Fan, H. J. Zhang, J. Y. Wang, L. L. Yu, Chem. Phys. Lett. 2006, **426**, 85-90.
[32]A. K. Parchur, A. A. Ansari, B. P. Singh, T. N. Hasan, F. N. Syed, S. B. Rai and R. S. Ningthoujam, Intger. Biol., 2014, **6**, 53-64.

[33]P. G. Zverev Phys. Status Solidi C 2004, **1**, 3101-3105.
[34]A. P. A. Marques, F. V. Motta, E. R. Leite, P. S. Pizani, J. A. Varela; E. Longo; de, D. M. A. de Melo, J. Appl. Phys. 2008, **104**, 043505-043510.
[35]S. I. Woo, J. S. Kim and H. K. Jun, J. Phys. Chem. B, 2004, **108**, 8941-8946.
[36]L. R. Shah, B. Ali, H. Zhu, W. G. Wang, Y. Q. Song, H. W. Zhang, S. I. Shah, J. Q. Xiao, J. Phys.: Condens. Matter, 2009, **21**, 486004-1-9.
[37]A. K. Parchur, A. I. Prasad, S. B. Rai, R. Tewari, R. K. Sahu, G. S. Okram, R. A. Singh and R. S. Ningthoujam, AIP Adv., 2012, **2**, 032119-1-17.
[38]Y. Vahidshad, M. N. Tahir, A. I. Zad, S. M. Mirkazemi, R. Ghazemzadeh and W. Tremel, J. Mater. Chem, C, 2015, **3**, 889-898.
[39]C. Hsu and R. C. Powell, Phys. Rev. Lett., 1975, **35**,734–737
[40]G. S. R. Raju, E. Pavitra, Y. H. Ko, J. S.Yu, J. Mater. Chem., 2012, **22**, 15562-15569.
[41]J. Yu, K. Huang, L.Yuan and S. Feng, New J. Chem., 2014, **38**, 1441-1445.
[42]T. Jia, Y. Liu, H. Zhao, H. Du, J. Sun and G. Ge, J. Solid State Chem., 2010, **183**, 584-589
[43] L. Sun, C. Qian, C. Liao, X. Wang and C. Yan, Solid State Commun., 2001, **119**, 393-396.
[44]L. P. Singh, S. K. Srivastava, R. Mishra, and R. S. Ningthoujam, J. Phys. Chem. C 2014, **118**, 18087−18096.
[45] K. K. Haldar, S. Kundu and A. Patra, Appl. Phys. Lett., 2014, **104**, 063110.